Conception of an Integrated Sensor for the Radiation Monitoring of the CMS Experiment at the Large Hadron Collider

F. Ravotti, *Student Member, IEEE*, M. Glaser, M. Moll, K. Idri, *Student Member, IEEE*, J. R. Vaillé, *Student Member, IEEE*, H. Prevost, and L. Dusseau, *Senior Member, IEEE*

***Abstract*—The concept of an active integrated dosimetric sensor for the radiation monitoring of the Compact Muon Solenoid experiment at the CERN (European Center for Nuclear Research) Large Hadron Collider is presented. The sensor, based on RadFET, OSL, p-i-n diode, and pad detector dosimeters, will measure both ionizing and nonionizing energy losses in the harsh radiation environment produced by hadron interactions.**

***Index Terms*—Optically stimulated luminescence, p-i-n diode, particle beams, RadFET, real-time dosimetry.**

I. Introduction

THE radiation environment encountered in the Large Hadron Collider (LHC) experiments at CERN [1] will differ completely from standard applications in which existing dosimetric technologies are used.

The mixed radiation field in the Compact Muon Solenoid (CMS) experiment will be composed of neutrons, photons and charged hadrons. This complex field, which has been simulated by Monte Carlo codes [2], is due to particles generated by the proton-proton collisions and reaction products of these particles with the sub-detector material of the experiment itself. The proportion of the different particle species in the field will depend on the distance and on the angle with respect to the interaction point (i.e., the radiation environment is unique for each sub-detector constituting CMS). For example, in the EndCap electromagnetic calorimeter of CMS, the Total Ionizing Dose (TID) over a 10- year period is estimated to reach 100 kGy and a fast hadron fluence of about 10^{14} particles per square centimeter.

Such an environment represents a danger to all exposed detectors and electronic components. Due to radiation damage via ionizing energy losses (IEL), nonionizing energy losses (NIEL), and other various ageing radiation effects [3], the detectors will suffer a loss of performance over time. In addition, the risk of accidental radiation burst due to beam loss or bad beam tuning, has also to be taken into account. For these reasons it is important to constantly monitor the radiation levels.

The present concept for the radiation monitoring system of the CMS experiment is comprised of the so-called Beam Condition Monitor (BCM) [4], placed a few centimeters from the interaction point, and the sensors that are presented in this work located at larger radii.

The BCM is currently under development. It will essentially provide a measurement of the beam condition and the possibility to send a beam-abort request to the LHC machine in order to protect the sub-detectors from high radiation levels. Based on Monte Carlo simulations, it can also be used to estimate the radiation levels throughout the whole experiment.

However, to measure the CMS radiation field exactly, a set of active sensors is needed to verify the simulations and correlate the BCM readings with the radiation field in the different sub-detectors [5]. Moreover, the sensors will accomplish the following tasks:

1) check the integrity of the shielding;
2) act as a long term radiation monitor in some critical locations;
3) measure the radiation background together with the ionization chambers that will be placed in the experimental area around CMS [6].

The aim of the present work is to describe the results of our recent dosimeters characterization obtained on different existing technologies and the integration of these dosimeters into an active sensor that ensures a complete monitoring of the radiation field parameters. Recently, also other LHC experiments have expressed their interest in this kind of radiation monitoring, leading to a common effort with the formation of the CERN–RADMON working group [7].

RadFET and OSL dosimeters, two complementary technologies for ionizing radiation measurement, were tested. OSRAM BPW34F p-i-n silicon photodiodes [8] and silicon pad detectors were tested as monitors for nonionizing radiation.

In Section II, the principles of the different dosimeters are reviewed. In Section III, the proton and neutron Irradiation Facilities of the CERN Proton Synchrotron (PS), used for the experiments, are described. In Section IV the experimental results are summarized. Finally, the concept for the integration is outlined and our conclusions are given in Sections V and VI, respectively.

Manuscript received September 3, 2004.

F. Ravotti is with the Department TS-LEA-CMS, CERN, Geneva 23, CH-1211, Switzerland (e-mail: Federico.Ravotti@cern.ch).

M. Glaser and M. Moll are with the Department PH-TA1-SD, CERN, Geneva 23, CH-1211, Switzerland (e-mail: Maurice.Glaser@cern.ch).

L. Dusseau, H. Prevost, K. Idri, and J. R. Vaillé are with CEM^2, Université Montpellier II, 34095 Montpellier Cedex 5, France (e-mail: dusseau@cem2.univ-montp2.fr).

Digital Object Identifier 10.1109/TNS.2004.839265

II. Review of the Dosimetric Technologies

A. Radiation-Sensitive Field Effect Transistors (RadFETs)

The RadFET dosimeters are p-channel MOS transistors that are used to measure ionizing dose by the build-up of charge in the SiO_2 layer of the device. The shift of transistor gate threshold voltage V_{th}, which is measured at a constant *source-drain* current, is proportional to the dose deposited in the gate insulator [9].

RadFETs are integrating devices in which the dosimetric information is kept stored even after every read out but they do not offer the sensitivity to measure very small doses ($<$ cGy). Moreover, the sensitivity decreases with increasing dose. Therefore, these devices are used when regular measurements of doses absorbed over long periods of time are required [10], [11].

B. Optically Stimulated Luminescence (OSL)

The property of irradiated OSL material to emit visible light proportional to the received dose is extensively described in references [12]–[14].

Ionizing radiation creates a large number of electron-hole pairs in the OSL material. A fraction of these carriers is trapped by dopants with energy levels located in the wide band gap of the insulator. Some of these charges will remain trapped for a period of time depending on the activation energy of the traps and the temperature. The energy necessary to release the charges is provided by an optical stimulation, and a subsequent radiative recombination may be observed. Quantifying the amount of the emitted light makes it possible to evaluate the dose [15].

The OSL has a higher sensitivity than RadFETs. The dosimetric information is however erased after every read-out and to obtain the dose absorbed over a long time it is thus necessary to add up all the readings. Complementary to the long-time integration of the RadFETs, the OSLs will therefore be used to detect very small increases of dose over short periods of time (e.g., days).

C. OSRAM BPW34F p-i-n Silicon Diodes

The BPW34F p-i-n photodiodes are junction devices with a base of high resistivity (some k$\Omega \cdot$ cm) n-type silicon with a thickness of a few hundred micrometers. They are cheap commercial devices designed for infrared remote control [8] and are sensitive to particle fluence due to displacement damage effects. In particular, they show an increase of their leakage current when biased reversely and a linear increase of their resistivity when powered forward [16], [17].

D. Pad Detectors (Reverse Biased p-i-n Diodes)

Silicon particle detectors are reverse biased p-i-n diodes with a very high resistivity (several k$\Omega \cdot$ cm) n-type bulk of usually 300 μm thickness. Irradiation of such devices will produce generation/recombination centers in the silicon bulk leading to a fluence proportional increase of the leakage current if the device is kept fully depleted. It has been demonstrated that the increase of the leakage current is independent from the impurity content of the silicon base material [18]. They can be used as a NIEL proportional damage counter for a wide range of different particles and particle energies if care is taken about the rather complex annealing behavior [19]. For dosimetric purposes usually small "pad structures" with an active area in the order of 0.25 to 1 cm^2 protected by one or several guard rings against edge currents are used.

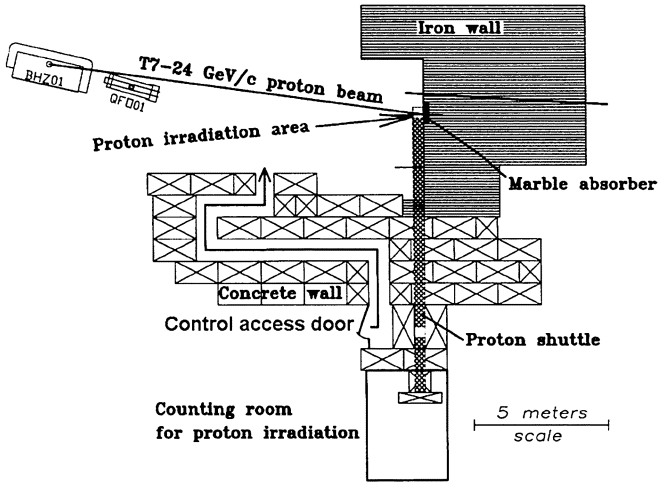

Fig. 1. Layout of the IRRAD1 irradiation facility.

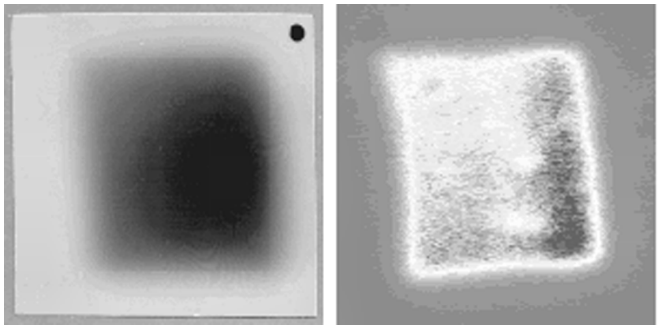

Fig. 2. Left: Beam spot on a 5 $\times$ 5 cm^2 Gafchromic XR sensitive film. Right: High-resolution 5 $\times$ 5 cm^2 beam profile measured by a 100 μm OSL film.

III. Irradiation Facilities and Dosimetry

A. CERN IRRAD1 24 GeV/c Proton Facility

Since 1998 the irradiation facility IRRAD1 has been operating in the East Hall Experimental Area of the CERN-PS complex. In the T7 beam-line, the primary 24 GeV/c proton beam is directed to the irradiation area, where a remote-controlled shuttle allows positioning of the samples to be irradiated by moving them from the counting room into the irradiation area, as shown in Fig. 1 [20].

The proton bursts are delivered during the 16.8 s supercycle of the PS in 1–3 spills of about 400 ms, with a maximum beam intensity of about 2×10^{11} protons per spill. A defocusing-scanning system is then used to spread out the beam in order to produce a uniform irradiation over a surface of several square centimeters as shown in Fig. 2.

The beam calibration and dosimetry during sample irradiation are performed with Gafchromic (Gafchromic is a registered trademark of ISP Corporation) sensitive films [21] and thin OSL films (when high resolution is needed in the determination of the

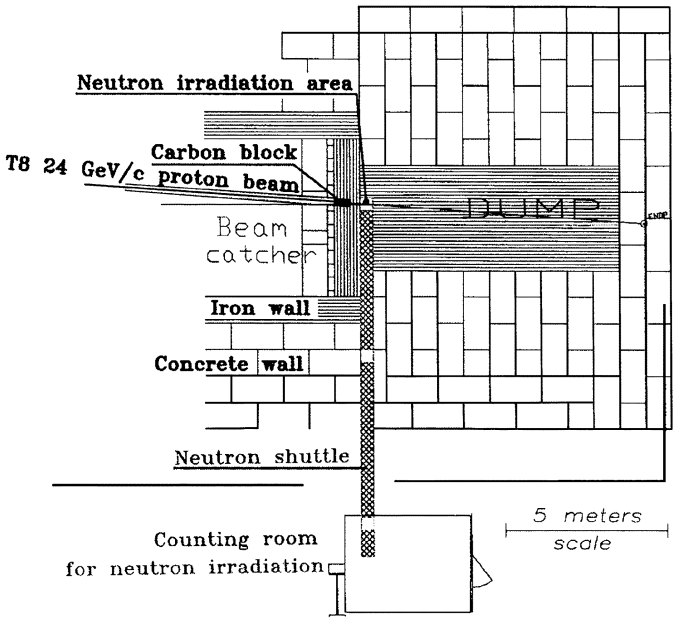

Fig. 3. Layout of the IRRAD2 irradiation facility.

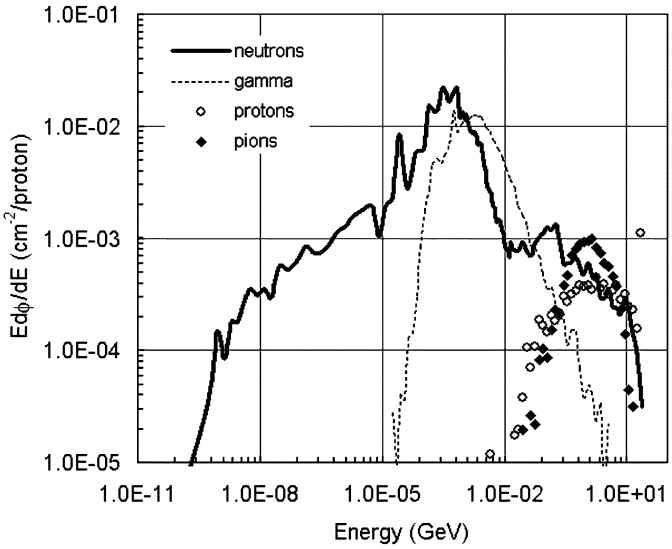

Fig. 4. Particle spectra in IRRAD2 cavity at 10 cm from beam axis normalized to one impinging 24 GeV/c proton.

dose mapping) [14]. The proton fluence is measured by evaluating the ^{24}Na activity of aluminum foils produced via the nuclear reaction $^{27}\mathrm{Al}(p,X)^{24}\mathrm{Na}$. With the latter technique it is possible to obtain fluence measurements with an accuracy of $\pm 7\%$. Taking into account that ionization is the main contribution to the energy loss of a charged particle and that its mean value, the stopping power (dE/dx) is given by the Bethe–Bloch law, it is possible to convert the fluence into the dose (Gy) deposited in thin samples, using the following formula:

$$D = K \times (dE/dx)_m \times \Phi \tag{1}$$

where Φ is the proton fluence expressed in $\mathrm{p/cm^2}$, $K = 1.602 \times 10^{-10}$ is a scale factor, and $(dE/dx)_m$, expressed in MeV $\cdot$ $\mathrm{cm^2/g}$, is the minimum ionizing energy loss rate. For GeV protons it assumes values between 1.6–1.8 MeV $\cdot$ $\mathrm{cm^2/g}$ for our materials. For high-energy charged particles, the contribution of nuclear interactions and the resulting secondaries to the dose in the beam is usually small and so it can be neglected under normal circumstances [22].

B. CERN IRRAD2 Mixed Gamma/Neutron Facility

Fig. 3 shows the layout of the irradiation zone IRRAD2 in the T8 beam-line. The irradiation is performed in a cavity with secondary particles produced by the primary 24 GeV/c proton beam crossing a thick beam dump consisting of carbon and iron blocks [20].

As for the IRRAD1 facility, a motorized shuttle system allows transport of samples from the counting room to the irradiation cavity in which a broad spectrum of neutrons and gamma rays is produced as shown in the spectra obtained by Monte Carlo simulations in Fig. 4 [23].

With the remote shuttle system, it is possible to set the position of the samples with respect to the beam axis. Depending on the position, the ratio of charged hadrons in the GeV energy range to neutrons and gammas can be chosen. It is thus possible to perform irradiations in a pure gamma/neutron environment (at positions far from the beam axis) or in a charged-hadron-rich radiation environment that better represents the one expected for the inner part of the LHC experiments (at positions close to the beam axis).

Different dosimetry techniques are used to monitor the neutron fluence and the deposited TID in this complex environment depending on the irradiation position and upon the users' request. For the present work, in which all the samples were placed in the pure neutron environment, calculations based on simulations [23], [24] as well as measurements with alanine [25] and silicon detectors [18] were used. With these techniques it is possible to obtain fluence measurements with an accuracy of $\pm 10\%$.

IV. Results and Discussion

In the present section, the results obtained during the characterization of the various technologies are summarized. Integration issues of all these technologies into one module will be presented in Section V.

A. Ionizing Radiation Measurement With RadFETs

RadFETs from different manufacturers and with various oxide thicknesses (0.1–0.85 μm) have been under investigation at CERN since the year 2001 [26], [27]. In order to provide the CMS experiment also with RadFETs for low dose ranges of up to some tens of Gy, our latest test campaign was focused on the study of devices with thicker oxide (1.6 μm) supplied by the *Laboratoire d'Analyse et d'Architecture des Systèmes* (LAAS), Toulouse, France.

The increase of the MOS threshold voltage under 100 μA drain current was read out in real-time at the end of a 25-m-long cable by a PC-controlled Keithley 2410 SourceMeter. The system was programmed to perform serial measurements in order to record a signal versus dose curve.

Fig. 5 shows the growth of the MOS threshold voltage versus dose (averaged over 2 to 4 identical devices measured at the

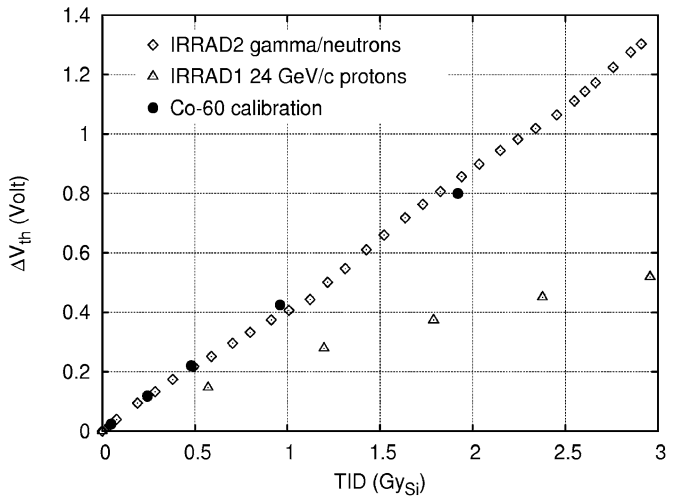

Fig. 5. Experimental results for LAAS devices obtained at CERN facilities.

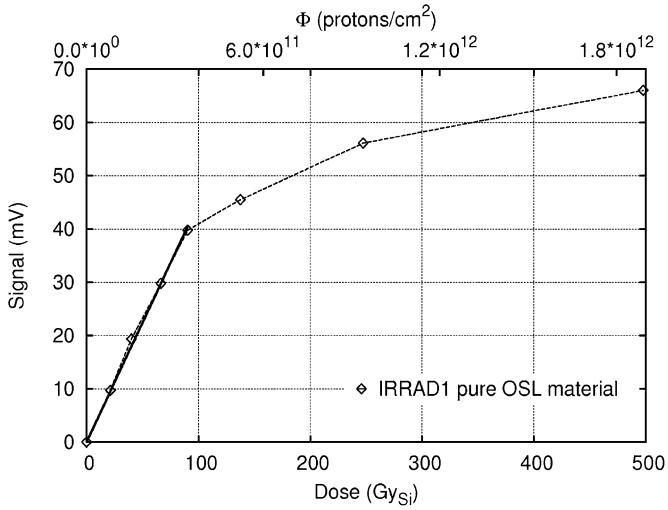

Fig. 6. Pure OSL material responses measured at IRRAD1.

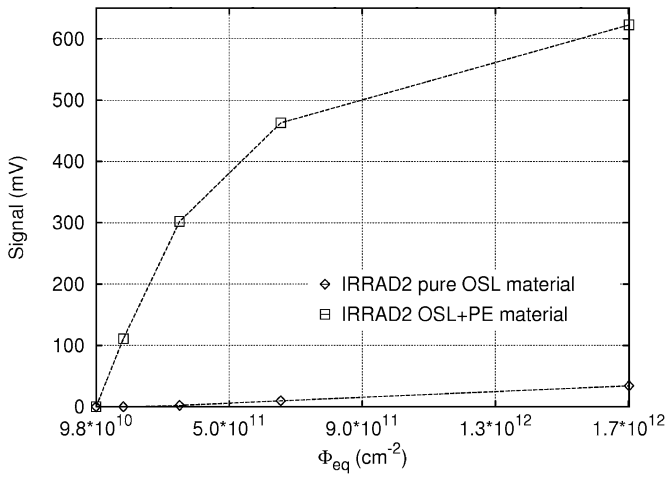

Fig. 7. OSL material responses as read from the test bench at IRRAD2.

same time) compared to the ^{60}Co calibration curve supplied by the manufacturer. For the IRRAD1 (24 GeV/c protons) data the dose is calculated from the proton fluence according to (1). For the IRRAD2 data the presented dose is the TID as calculated from a FLUKA simulation [23], [24] including the neutron contribution to ionizing KERMA (Kinetic Energy Released in MAterial) that was estimated to be a few percent. The maximum value of 3.0 $\mathrm{Gy_{Si}}$ corresponds to a 1-MeV neutron equivalent fluence of 1.1×10^{12} particles per square centimeter.

The response measured in the IRRAD2 facility fits exactly the calibration curve indicating that the simulation estimates predict the ionization due to neutrons correctly [28]. The measured high sensitivity of 4.2 mV/cGy, defined as the slope of the signal versus dose in its initial linear region, will allow use of these devices as high accuracy dosimeters in regions of the experiments where the expected doses will be less than 3 $\mathrm{Gy_{Si}}$[29].

However, the voltage shift measured in IRRAD1 is already reduced by a factor of 2.4 at the maximum dose of 3 $\mathrm{Gy_{Si}}$ considered here. This phenomenon, probably due to recombination processes within the SiO_2 layer [30], has to be carefully taken into account, if the devices have to be used in regions of the experiments that are dominated by high-energy charged particles.

The annealing of the RadFET signal with time and temperature has been investigated and is presented in [27]. It was found that the annealing of the trapped charge at room temperature was varying strongly in RadFETs supplied by different producers. The signal loss ranged from 20% in a few hours to 1% in a few months. A more detailed characterization of all types of RadFETs tested at CERN using an isochronal annealing technique [31] is presently under way.

B. Ionizing Radiation Measurement With OSLs

Besides the beam profile characterization shown in Section III, two types of experiments were carried out with the OSL. Pure OSL materials, as well as different samples doped with boron or mixed with polyethylene (PE) were produced in order to increase the OSL's sensitivity to a wide neutron spectrum.

A preliminary characterization was performed with high-energy protons and in the mixed gamma/neutron field at IRRAD1 and IRRAD2, respectively. In order to prove the reproducibility of the results, for each particle fluence 3 to 5 pieces of each type of OSL material were irradiated.

The results, obtained by reading the samples after irradiation with a laboratory test bench [14], are presented in Figs. 6 and 7.

The diamond marks of Fig. 6 represent the response of the pure OSL material to the 24 GeV/c proton beam in the explored dose range up to 500 $\mathrm{Gy_{Si}}$, corresponding to a fluence of 1.9×10^{12} $\mathrm{p/cm^2}$. The measurements were taken with a pure OSL sample that was successively irradiated to the indicated proton fluences. The response follows a linear behavior up to almost 100 $\mathrm{Gy_{Si}}$, becoming sub-linear due to saturation at higher doses.

The IRRAD2 irradiations plotted in Fig. 7 were performed with samples of different composition. For values of neutron equivalent fluence under 1.0×10^{11} $\mathrm{cm^{-2}}$, the signal was below the noise level since the gain of the read out system was set to measure high doses. The pure OSL material (diamond marks) shows insensitivity to the neutron component of the field and the measured signal is compatible with the TID predicted by the simulation. The polyethylene-enriched samples (square marks) show a factor 20 increase in sensitivity.

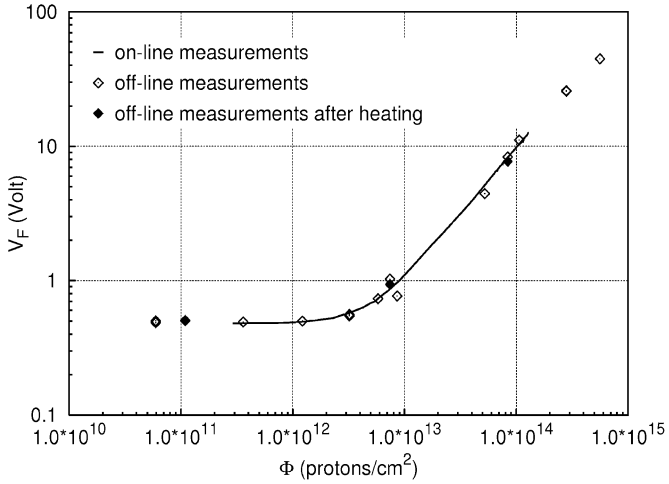

Fig. 8. Comparison between the results obtained for the BPW34F diodes in on-line and off-line mode at IRRAD1. The forward voltage is plotted against the proton fluence.

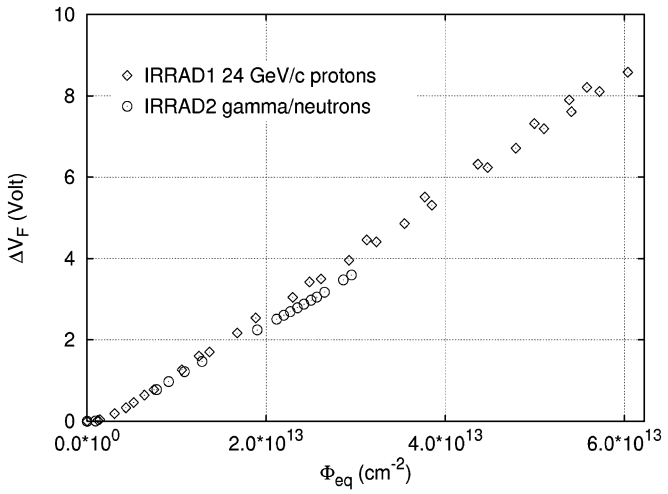

Fig. 9. Shift of the forward voltage for BPW34F devices obtained at CERN facilities and expressed in terms of 1-MeV neutron equivalent fluence.

The results of the boron-doped samples are published elsewhere [32]. They show very low responses on the same order of the pure OSL material ones which is in agreement with the fact that the thermal neutron component of the IRRAD2 spectrum is essentially zero (see Fig. 4).

Furthermore, an OSL sensor, developed for space applications [15], was tested. The device, placed in the beam, was connected by a 30-m-long coaxial cable to the read out system. Although it was possible to record an OSL signal, it appeared that the associated electronics of the sensor, as developed for space applications, was not suited to our experiment in terms of radiation hardness and signal read out over long cables.

For the integrated sensor presented in this article, a new approach, better adapted to the specifications of the CMS environment is currently under development and will be presented in Section V.

C. Nonionizing Radiation Measurement With BPW34F

The possibility to use the BPW34F semiconductor diodes as dosimeters was investigated at CERN several years ago [33]. In order to better characterize these devices, we performed further proton and neutron irradiations, measuring the voltage drop for a fixed forward current on- and off- line (i.e., during irradiation and in the laboratory).

With the same readout electronics used for RadFETs, a short pulse of 1 mA was injected for 180 ms, and the corresponding forward voltage $(V_{\rm F})$ was read out. This technique was applied to avoid current induced annealing phenomena. The pre-irradiation analysis shows a large temperature coefficient of about -40 mV/°C. Therefore, the temperature was monitored during the experiments and its dependence taken into account.

In Figs. 8 and 9 the obtained results are presented. Different proton fluxes from 2.2×10^{9} cm^{-2} to 3.1×10^{10} cm^{-2} per spill have been used in the IRRAD1 facility. However, no differences regarding the response of the dosimeters were observed.

In Fig. 8 the on-line measurements are compared to the data taken after irradiation (off-line). A part of the data were taken directly after irradiation while some of the data were measured after a heating of 4 min at 80 °C in order to simulate annealing of the devices at room temperature. Although further experiments are needed to study the annealing behavior in detail, this first test already indicates that the annealing is not a severe problem for off-line measurements.

To allow a comparison of the IRRAD1 data with the results obtained in the IRRAD2 facility, the proton fluence in Fig. 9 was converted into the 1-MeV neutron equivalent fluence by means of the hardness factor of 0.62 [19].

After an initial flat region up to a neutron equivalent fluence of 1.0×10^{12} cm^{-2}, at which the devices are not sensitive, the response is linear and in good agreement with the displacement damage scaling in silicon as shown in Fig. 9. A forward voltage shift of 1.1 V was measured for a neutron equivalent fluence of 10^{13} cm^{-2}. With the above characteristics, these devices are usable to measure high fluences, but the possibility to monitor also the reverse currents, leaves the way open to extend the sensitivity of these devices into the low fluence range. The influence of the forward current pulse length and the relatively weak annealing are currently under study.

D. Nonionizing Radiation Measurement With Pad Detectors

In this work, 307-μm-thick p-i-n detector test structures produced by ST Microelectronics, Italy, with an active area of 0.25 cm^2 and protected on the front side by a guard ring from edge currents have been used. The detectors were exposed to the different radiation fields at ambient temperature (about 27 °C) without biasing them. After irradiation the devices were annealed for 4 min at 80 °C and the leakage current at full depletion was measured and normalized to 20 °C (see, e.g., [19]). The results are presented in Fig. 10 and demonstrate that these devices can be used over a very wide fluence range provided that the annealing is performed carefully.

V. Dosimeters Integration

From the above results, it is clear that the four different technologies can provide a complete and quantitative map of the complex radiation environments. Moreover, the four types of

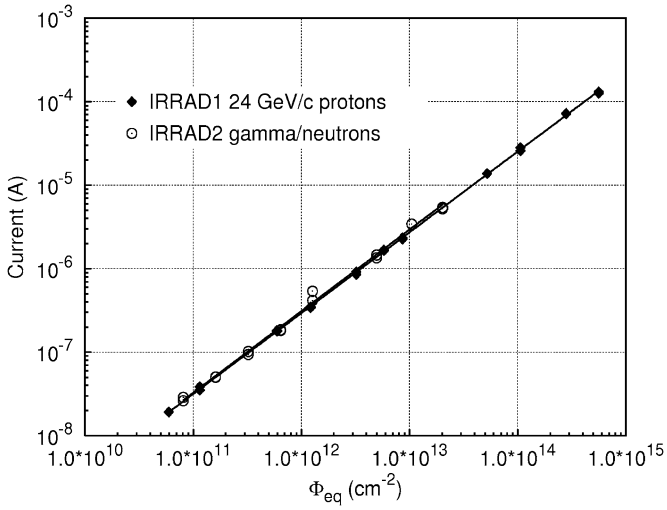

Fig. 10. Increase of the pad detector leakage current versus the 1-MeV neutron equivalent fluence.

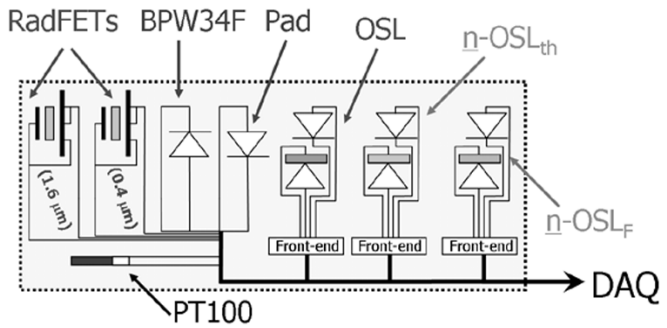

Fig. 11. Layout of the integrated sensor board prototype for the 2004 irradiation campaign at CERN. From the left to the right: RadFETs with different oxide thicknesses to cover different sensitivity ranges, p-i-n diodes for the measurement of the forward and reverse current, pure OSL materials, boron doped OSLs ($\underline{n}$-OSL$_{th}$) for thermal neutron measurement and OSL materials mixed with paraffin ($\underline{n}$-OSL$_{th}$) for fast neutron detection.

devices have sensitive areas of a few square millimeters only and can be read out over long distances.

Thus, they can be integrated into a dosimeter board which fulfills the requirements for the radiation monitoring of the CMS experiment or other LHC experiments. The dosimeters, together with a temperature probe PT100 and front-end electronics for the OSLs (current amplifier with line driver) could be integrated on a single PCB. The conceptual design of the PCB for the first prototype of the sensor is shown in Fig. 11.

The implementation of the RadFETs and the p-i-n diodes is straight forward while the integration of the OSLs still needs some development. In particular new specimens of pure and neutron-sensitive OSLs have already been prepared. To improve the light collection efficiency of the OSL dosimeters, pure OSL and boron-doped OSL materials have been deposed directly on the active surface of GaAsP visible photodiodes sealed in a TO-5 packages. For fast-neutron detection the package of some OSL pure samples were filled up with paraffin.

The purpose of a first prototype is to prove the reliability of a long-term, on-line readout in a typical accelerator mixed radiation field. The size, the material budget and the radiation hardness of the PCB and its components are considered as important constraints and are under definition. The sensor PCB will be installed in the T7 beam-line irradiation area (see Fig. 1) in the near future.

VI. Conclusion

The radiation monitoring of the CMS experiment at the CERN Large Hadron Collider is a challenging issue due to the complexity, intensity, and composition of its radiation field.

The experimental results obtained at the CERN-PS Irradiation Facilities on the four different tested dosimeter technologies, which are being used to monitor both ionizing (RadFETs and OSLs) and nonionizing energy losses (BPW34F p-i-n diodes and pad detectors), were briefly summarized. The promising results make the concept of an integrated radiation sensor an attractive approach. A first prototype sensor has been designed and is now ready to be tested.

Acknowledgment

The authors wish to thank E. Tsesmelis and C. Joram from CERN for clarifying discussions and valuable comments during the preparation of this paper, G. Sarrabayrouse from CNRS-LAAS for providing the MOS dosimeters, and A. Helienek from University of Vienna for her help in the p-i-n diodes characterization. The CERN TS-LEA group is also gratefully acknowledged for its general support.

References

[1] The Large Hadron Collider Project Webpage. [Online]. Available: http://cern.ch/lhc-new-homepage/

[2] M. Huhtinen, "Radiation environment simulations for the CMS detector," CERN, CMS Tech. Note 95-198, 1995.

[3] A. G. Holmes-Siedle and L. Adams, *Handbook of Radiation Effects*, 2nd ed. Oxford, U.K.: Oxford University Press, 2002.

[4] L. Fernandez-Hernando, C. Ilgner, A. Macpherson, A. Oh, H. Pernegger, T. Pritchard, and R. Stone, "A beam condition monitor for the experimental areas of the LHC," presented at the 9th Eur. Particle Accelerator Conf. (EPAC 2004), Lucerne, Switzerland, July 2004.

[5] M. Huhtinen, "Proposal for a radiation monitoring system," presented at the 3rd CMS Radiation Monitoring Meeting, May 2003, [Online.] Available: http://cern.ch/lhc-expt-radmon.

[6] D. Forkel-Wirth, D. Perrin, L. Scibile, G. Segura, F. Szoncso, and P. Vojtyla, "Radiation monitoring system for the environment and safety (RAMSES)—Functional specification," CERN, LHC Project Document LHC-P-ES-0003, 2003.

[7] RADMON. CERN, LHC Experiment Radiation Monitoring Working Group. [Online]. Available: http://cern.ch/lhc-expt-radmon/

[8] BPW34F Photodiode Datasheet. OSRAM Opto-Semiconductors. [Online]. Available: http://www.osram-os.com

[9] B. Camanzi, A. G. Holmes-Siedle, and A. K. McKemey, "The dose mapping system for the electromagnetic calorimeter of the BaBar experiment at SLAC," *Nucl. Inst. Meth.*, vol. A457, pp. 476–486, 2001.

[10] B. O'Connell, C. Connelly, C. McCarthy, J. Doyle, W. Lane, and L. Adams, "Electrical performances and radiation sensitivity of stacked PMOS dosimeters under bulkbias control," *IEEE Trans. Nucl. Sci.*, vol. 45, pp. 2689–2694, 1998.

[11] A. G. Holmes-Siedle and L. Adams, "RadFETs: A review of the use of metal-oxide-silicon device as integrating dosimeters," *Rad. Phys. Chem.*, vol. 28, no. 2, pp. 235–244, 1986.

[12] O. Missous, F. Loup, J. Fesquet, H. Prevost, and J. Gasiot, "Optically stimulated luminescence of rare-earth doped phosphors," *Eur. J. Solid State Inorg. Chem.*, vol. 28/s, pp. 163–166, 1991.

[13] D. Plattard, G. Ranchoux, L. Dusseau, G. Polge, J-R. Vaillé, J. Gasiot, J. Fesquet, R. Ecoffet, and N. Iborra-Brassart, "Characterization of an integrated sensor using optically stimulate luminescence for in-flight dosimetry," *IEEE Trans. Nucl. Sci.*, vol. 49, pp. 1322–1326, 2002.

[14] L. Dusseau, G. Polge, S. Matias, J.R. Vaillé, R. Germanicus, R. Broadhead, B. Camanzi, M. Glaser, F. Saigne, J. Fesquet, and J. Gasiot, "High-energy particle irradiation of optically stimulated luminescent films at CERN," *IEEE Trans. Nucl. Sci.*, vol. 48, pp. 2056–2066, 2001.

[15] L. Dusseau, J.R. Vaillé, S. Ducret, K. Idri, S. Matias, N. Iborra, F. Saigne, R. Germanicus, and R. Ecoffet, "Hardening of a radiation sensor based on optically stimulated luminescence," *IEEE Trans. Nucl. Sci.*, vol. 50, pp. 2358–2362, 2003.

[16] A.B. Rosenfeld *et al.*, "PIN diodes with a wide measurements range of fast neutron dose," *Rad. Prot. Dos.*, vol. 33, no. 1–4, pp. 175–178, 1990.

[17] Z. Li, W. Chen, and H. W. Kraner, "Effects of fast neutron radiation on the electrical proprieties of silicon detectors," *Nucl. Inst. Meth.*, vol. A308, pp. 585–595, 1991.

[18] M. Moll, E. Fretwurst, and G. Lindström, "Leakage current of hadron irradiated silicon detectors—Material dependence," *Nucl. Inst. Meth.*, vol. A426, pp. 87–93, 1999.

[19] M. Moll, E. Fretwurst, M. Kuhnke, and G. Lindström, "Relation between microscopic defects and macroscopic changes in silicon detector properties after hadron irradiation," *Nucl. Inst. Meth.*, vol. B186, pp. 100–110, 2002.

[20] M. Glaser, L. Durieu, F. Lemeilleur, M. Tavlet, C. Leroy, and P. Roy, "New irradiation zones at the CERN-PS," *Nucl. Inst. Meth.*, vol. A426, pp. 72–77, 1999.

[21] GAFCHROMIC® Radiochromic Dosimetry Films Datasheets. ISP. [Online]. Available: http://www.ispcorp.com

[22] A. H. Sullivan, *A Guide to Radiation and Radioactivity Levels Near High-Energy Particle Accelerators*. London, U.K.: Nuclear Technology Pub., 1992.

[23] M. Huhtinen, private communication, CERN PH Dept., Geneva, Switzerland, 2003.

[24] H. Vincke, I. Brunner, and M. Huhtinen, "Production of radioactive isotopes in Al, Fe, Cu-Samples by stray radiation fields at proton accelerator," CERN, CERN-TIS-2002-007-RP, 2002.

[25] F. Coninckx, H. Schonbacher, M. Tavlet, G. Paic, and D. Razem, "Comparison of high-dose dosimetry systems for radiation damage studies in collider detectors and accelerators," *Nucl. Inst. Meth.*, vol. B83, pp. 181–188, 1993.

[26] B. Camanzi, M. Glaser, E. Tsesmelis, and L. Adams, "A study on the applicability of solid-state, real-time dosimeters to the CMS experiment at the large hadron collider," *Nucl. Inst. Meth.*, vol. A500, pp. 431–440, 2003.

[27] F. Ravotti and M. Glaser, "A Study of the response of solid-state dosimeters to be used for the measurement of the radiation environment of the CMS experiment at the LHC," CERN, CERN EST Tech. Note EST-LEA/2003-03, 2003.

[28] S. Kronenberg and G. J. Brucker, "The use of hydrogenous material for sensitizing pMOS dosimeters to neutrons," *IEEE Trans. Nucl. Sci.*, vol. 42, pp. 20–26, 1995.

[29] G. Sarrabayrouse and V. Polischuk, "MOS ionizing radiation dosimeters: From low to high dose measurement," *Rad. Phy. Chem.*, vol. 61, pp. 511–513, 2001.

[30] R. Pease, M. Simons, and P. Marshall, "Comparison of pMOS total dose response for Co-60 gammas and high-energy protons," *IEEE Trans. Nucl. Sci*, vol. 48, pp. 908–912, 2001.

[31] F. Saigne, L. Dusseau, J. Fesquet, J. Gasiot, R. Ecoffet, R. D. Schrimpf, and K. F. Galloway, "Evaluation of MOS devices' total dose response using the isochronal annealing method," *IEEE Trans. Nucl. Sci.*, vol. 48, pp. 2170–2173, 2001.

[32] F. Ravotti, M. Glaser, K. Idri, J-R. Vaillé, H. Prevost, and L. Dusseau, "Optically stimulated luminescence materials for wide-spectrum neutron measurement at CERN," presented at the RADECS 2004 Workshop, Madrid, Spain, Sept. 2004, CERN-PH-EP-2004-022.

[33] A. Rosenfeld, V. Khivrich, V. Kuts, M. Tavlet, L. Malfante, and C. Munoz-Ferrada, "Use of Ukrainian semiconductor dosimeters in a CERN particle accelerator field," *IEEE Trans. Nucl. Sci.*, vol. 41, pp. 1009–1013, 1994.